

Probing interactions between HIV-1 reverse transcriptase and its DNA substrate with backbone-modified nucleotides

Andreas Marx¹, Martin Spichty¹, Mario Amacker², Urs Schwitter¹, Ulrich Hübscher², Thomas A Bickle³, Giovanni Maga⁴ and Bernd Giese¹

Background: To gain a molecular understanding of a biochemical process, the crystal structure of enzymes that catalyze the reactions involved is extremely helpful. Often the question arises whether conformations obtained in this way appropriately reflect the reactivity of enzymes, however. Rates that characterize transitions are therefore compulsory experiments for the elucidation of the reaction mechanism. Such experiments have been performed for the reverse transcriptase of the type 1 human immunodeficiency virus (HIV-1 RT).

Results: We have developed a methodology to monitor the interplay between HIV-1 RT and its DNA substrate. To probe the protein–DNA interactions, the sugar backbone of one nucleotide was modified by a substituent that influenced the efficiency of the chain elongation in a characteristic way. We found that strand elongation after incorporation of the modified nucleotide follows a discontinuous efficiency for the first four nucleotides. The reaction efficiencies could be correlated with the distance between the sugar substituent and the enzyme. The model was confirmed by kinetic experiments with HIV-1 RT mutants.

Conclusions: Experiments with HIV-1 RT demonstrate that strand-elongation efficiency using a modified nucleotide correlates well with distances between the DNA substrate and the enzyme. The functional group at the modified nucleotides acts as an ‘antenna’ for steric interactions that changes the optimal transition state. Kinetic experiments in combination with backbone-modified nucleotides can therefore be used to gain structural information about reverse transcriptases and DNA polymerases.

Introduction

The reverse transcriptase (RT) of the human immunodeficiency virus type 1 (HIV-1) copies the single-stranded RNA genome of the retrovirus into double-stranded DNA [1]. This is an essential step in the retroviral life cycle. HIV-1 RT is widely targeted by many clinically approved drugs to combat AIDS [2] and much knowledge of its structure and function has been gained recently. A crystal structure of HIV-1 RT complexed with the inhibitor nevirapine suggests that the RT is an asymmetric dimer (p66/p51) in which the polymerase domain of the 66 kDa subunit has a large cleft analogous to that of the Klenow fragment of *Escherichia coli* DNA polymerase I [3]. More insights into the interactions of the protein with the primer–template complex were gained through the determination of crystal structures of a ternary complex between HIV-1 RT, double-stranded DNA template–primer and a monoclonal antibody Fab fragment [4], and, more recently, from a complex of HIV-1 RT covalently linked to double-stranded DNA template–primer and a 2′-deoxynucleotide triphosphate [5]. These structures suggest that the most numerous

nucleic-acid interactions with the protein occur primarily along the sugar–phosphate backbone of the DNA. We developed a method in which these interactions can be probed by the use of nucleotides that are modified at the sugar-phosphate backbone.

According to the crystal structures of HIV-1 RT complexed with double-stranded DNA, the $\beta 9$ – $\beta 10$ motif is involved in the correct alignment of the 3′ end of the primer terminus, as well as in the binding of the nucleotide triphosphate [6] (Figure 1). The $\beta 12$ – $\beta 13$ motif was designated the primer grip, proposing that it maintains the primer terminus in the appropriate orientation. Furthermore, the α H helix of the p66 thumb makes contacts with the sugar-phosphate backbone of the primer strand and might function as a track over which the primer–template complex moves during translocation.

The assumption that these protein–DNA interactions are crucial for DNA polymerization catalyzed by HIV-1 RT was further supported by studies using mutants of HIV-1

Addresses: ¹Department of Chemistry, University of Basel, St. Johannis-Ring 19, CH-4056 Basel, Switzerland. ²Department of Veterinary Biochemistry, University of Zürich, Winterthurerstrasse 190, CH-8057 Zürich, Switzerland. ³Division of Molecular Microbiology, Biozentrum, University of Basel, Klingelbergstrasse 70, CH-4056 Basel, Switzerland. ⁴Istituto di Genetica Biochimica ed Evoluzionistica, Consiglio Nazionale della Ricerche, via Abbiategrosso 207, I-27100 Pavia, Italy.

Correspondence: Bernd Giese
E-mail: giese@ubaclu.unibas.ch

Key words: 4′-acylated thymidine triphosphate, DNA–protein interaction, DNA polymerase, HIV-1 reverse transcriptase

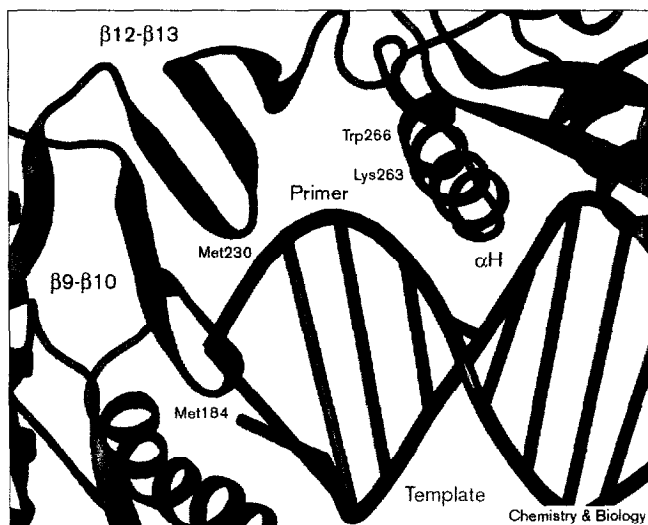
Received: 9 July 1998
Revisions requested: 29 July 1998
Revisions received: 24 November 1998
Accepted: 25 November 1998

Published: 21 January 1999

Chemistry & Biology February 1999, 6:111–116
<http://biomednet.com/elecref/1074552100600111>

© Elsevier Science Ltd ISSN 1074-5521

Figure 1



Polymerase active site of HIV-1 RT complexed with a DNA template-primer duplex. The enzyme backbone was built using the C α coordinates [4] (PDB entry 1HMI) and the program MOLOC 2.0 [21]. A ten-base DNA duplex with an overhanging nucleotide at the 5' terminus was modeled with MACROMODEL V4.5 (Department of Chemistry, Columbia University, New York, NY 10027 [22]) from the P-atom positions (given in [4]). The first six base pairs including the overhanging nucleotide were constructed in A form and the rest of the duplex in B form. The double-stranded DNA was optimized with AMBER force field [23] implemented in MACROMODEL V4.5. The enzyme backbone is shown in green ribbon model and the DNA duplex as bicoloured ladder. The red part represents the primer strand, whereas the purple part represents the template strand. The amino acids that are closest to the primer strand are shown. Structural elements near the primer strand are dark blue. Graphical layout was produced with PREPI V1.0 (Imperial Cancer Research Technology; <http://bonsai.lif.icnet.uk/people/suhail/prepi.html>).

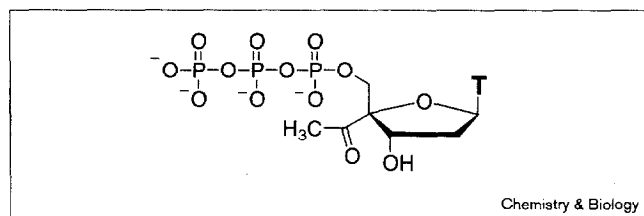
RT [7–10]. It remains uncertain, however, whether the crystal structures, which were obtained from crystals under nonoptimal conditions for the enzyme, appropriately reflect the action of the RT under conditions where the enzyme is in its active form. Our methodology provides a new insight into the function of HIV-1 RT in its active form and its resistance against nucleoside and non-nucleoside anti-HIV drugs caused by mutations of the enzyme.

Results and discussion

Chain elongation with wild-type HIV-1 RT

To probe the protein interactions with the sugar-phosphate backbone of a primer-template DNA complex we modified the sugar residue of a thymidine triphosphate at the 4' position by substituting the 4' hydrogen with an acetyl functionality (Figure 2) [11,12]. We expected an influence on the efficiency of phosphodiester-bond formation at any position along the DNA polymerization pathway where the 4' modification makes contact with any residue of the protein that is crucial for catalysis.

Figure 2



Structure of the backbone-modified thymidine triphosphate.

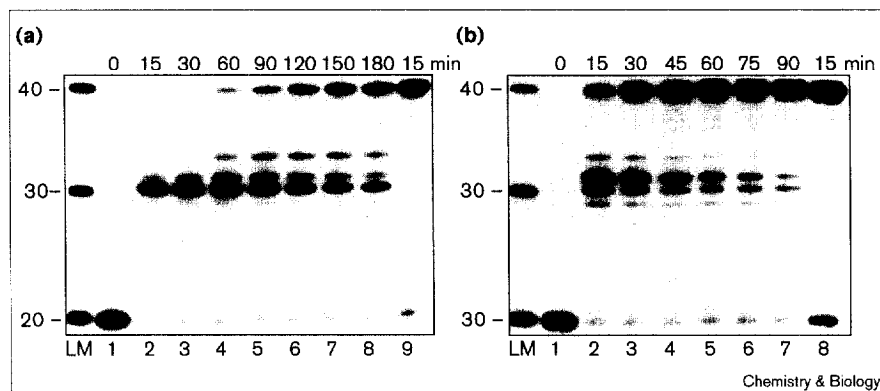
We have shown that HIV-1 RT is able to incorporate the backbone-modified thymidine triphosphate into the growing DNA strand [12]. In these experiments, we found that only 4'-acetyl thymidine has the right shape for incorporation and post-incorporation chain elongation in DNA-strand synthesis catalyzed by HIV-1 RT [12]. To probe the interactions of the 4' modification with the enzyme surface, we incubated HIV-1 RT with a DNA 5'-³²P-labelled 20-base primer/40-base template complex in which a single adenosine moiety in the template strand demands the incorporation of a thymidine analogue at position 30 in the presence of dATP, dCTP, dGTP and the 4'-acetylated thymidine triphosphate for various times, and analyzed the reaction products using polyacrylamide gel electrophoresis (PAGE; Figure 3a).

After incubation for 15 min, the formation of a 30-base reaction product indicated the complete incorporation of the 4'-acetyl thymidine analogue. With increasing time, the additional formation of 31- and 33-base products were observed prior to the formation of the full-length 40-base product. The formation of a 32-base reaction product was not detected in substantial amounts, indicating that elongation to the 33mer was rapid. The DNA products in the range of 30–40 bases obtained in these experiments were quantified using phosphorimaging techniques (Figure 4). The data in Figure 4a indicate that the DNA strand is elongated by HIV-1 RT after incorporation of the 4'-modified thymidine with a discontinuous efficiency of phosphodiester-bond formation for the first four nucleotides.

In order to verify that the band pattern obtained reflects the interaction of the backbone modification with the protein and does not result from a natural pausing site, the reaction was performed in the presence of thymidine triphosphate (TTP) instead of the modified analogue (Figure 3, lane 9). This does not lead to the formation of substantial amounts of reaction products shorter than the 40-base full-length product. Furthermore, to exclude the possibility that the base composition of the template is responsible for the discontinuous formation of reaction products, the base composition of the template, as well as the length of the primer-template complex was varied.

Figure 3

Effect of 4'-modified thymidine triphosphate on DNA strand synthesis catalyzed with HIV-1 RT. Shown is an autoradiogram of an 11% denaturing PAGE. The numbers on the left side indicate the length of oligonucleotide synthesized in primer extension. (a) LM, line marker; lanes 1–8, a 20-base DNA ^{32}P -5'-end labelled primer (15 nM, 5'-d(GTGGTGCGAAT-TCTGTGGAT)) and 40-base DNA template (45 nM, 5'-d(TCGGTCGTTTCATCCTTGCTGATCCACAGAATTCGCACCAC)), dATP, dGTP, dCTP (2 μM each), and the modified thymidine triphosphate (100 μM) incubated at 37°C for several times with HIV-1 RT (0.2 U/ μl) as indicated in the figure; lane 9, control reaction, as in lanes 1–8 but with TTP (100 μM) instead of the modified thymidine triphosphate and incubation for 15 min. (b) Lanes 1–7, same as in (a), but with HIV-1 RT Met184→Val mutant; lane 8, control reaction.



This did not effect any significant change in the elongation pattern (data not shown). Recently published experiments, in which the same assay was employed and primer extension reactions were performed either in the absence of any TTP analog or in the presence of the 4'-acylated TTP analogue clearly showed that under the employed conditions HIV-1 RT is able to incorporate the 4'-acylated TTP analog opposite to an adenosine moiety in favour of the misincorporation of another dNTP [12]. This indicates that the band pattern observed is due to the incorporation of the modified nucleotide.

Efficiency of chain elongations

In order to quantify the nucleotide-incorporation efficiency at various points of the DNA polymerization pathway we used a gel-based, steady-state kinetic assay [13,14] and

employed unmodified as well as 4'-acylated DNA primers (see the Materials and methods section). The kinetic data obtained for both sets of reactions are quite striking (Table 1). When unmodified primers were used in the HIV-1 RT catalyzed primer extension no significant variation in catalytic efficiency was observed in the region of investigation, whereas in primer extension of 4'-acylated primers discontinuous catalytic efficiency was observed. This demonstrates that the discontinuous efficiency of DNA synthesis observed when modified primers were employed is due to interactions of the modification with the enzyme surface and not to any natural variation in efficiency. Furthermore, it turned out that addition of the next nucleotide after incorporation of the 4'-modified thymidine is the least efficient step in the primer-extension pathway.

Figure 4

Comparison of the effect of 4'-acylated thymidines on DNA synthesis catalyzed by HIV-1 RT (wt, wild type) and HIV-1 RT (Met184→Val) mutant. Shown is the distribution of 30–40 base reaction products of the reactions presented in Figure 3 after several incubation times. The bars represent the proportion of radioactivity for a DNA reaction product to the entire radioactivity in the lane. The radioactivity was quantified using PhosphorImaging techniques.

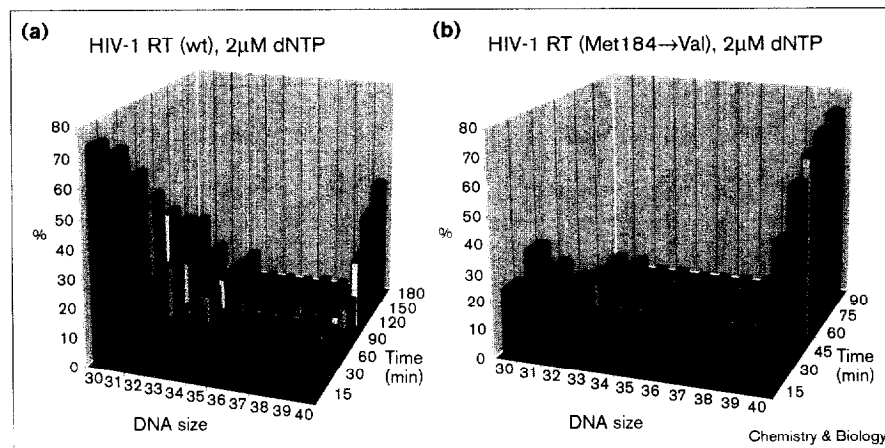


Table 1**DNA elongation efficiency of unmodified and 4'-modified primers catalyzed by HIV-1 RT (wt).**

Entry	Elongation event	Modified primer V_{\max}/K_M	Unmodified primer V_{\max}/K_M
1	30→31	3.8×10^{-3}	4.0×10^{-2}
2	31→32	1.6×10^{-2}	4.6×10^{-2}
3	32→33	1.0×10^{-1}	5.0×10^{-2}
4	33→34	2.4×10^{-2}	3.8×10^{-2}

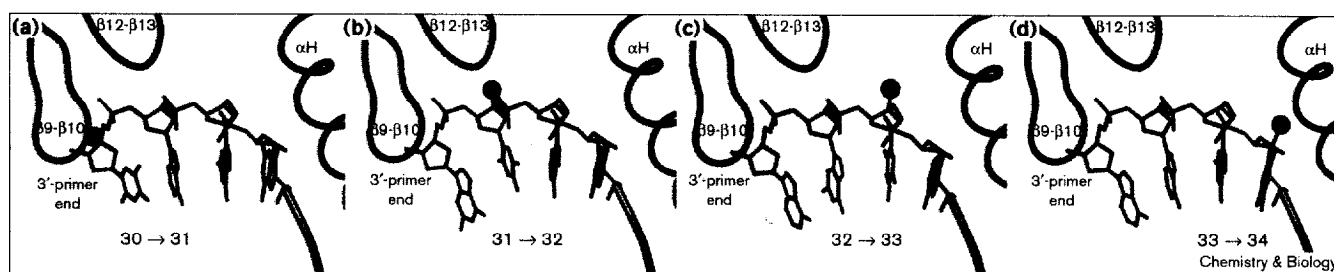
We explain this band pattern as different interactions of the 4' substituent at the nucleotide with different residues of the enzyme. The crystal structures of HIV-1 RT complexed with a double-stranded DNA substrate [4,5] suggest that the protein has very extensive contacts between the tip of the $\beta 9$ – $\beta 10$ hairpin (Met184) and the first nucleotide at the 3' end of the primer strand (Figure 1). The second nucleotide from the 3'-primer end contacts the primer grip $\beta 12$ – $\beta 13$ at Met230 (Figure 1). In both cases backbone modifications in the primer strand should have major interactions with these enzyme motifs because the rigid peptide backbone is in close vicinity to the primer (Figure 5a,b). These interactions might result in a misalignment of the modified DNA substrate in the enzyme cleft. This misalignment or a perturbed binding of the enzyme with the modified DNA substrate could lead to a less efficient phosphodiester-bond formation (Table 1, entries 1 and 2, modified primer). The third nucleotide downstream from the 3'-primer end is located farther away from the peptide backbone. The indole sidechain (Trp266, Figure 1) of the αH helix is in close contact to this nucleotide, however [5]. Nevertheless, a more efficient elongation of the modified primer occurs and only small amounts of a 32-base reaction product are observed (Figures 3a and 4a; Table 1, entry 3, modified primer). We assume that at this position the

repulsive interactions between the modified nucleotide and the enzyme can be avoided through rotation of the planar indole sidechain into the gap between the $\beta 12$ – $\beta 13$ and the αH motifs (Figure 5c). During further movement of the backbone modification through the polymerase cleft, interactions between the enzyme and the DNA primer-template sugar-phosphate backbone occur with the αH helix and the fourth nucleotide from the 3'-primer end (Figure 5d). The efficiency is therefore reduced again (Table 1, entry 4, modified primer) and a 33-base reaction product accumulates.

Reactions with mutants of HIV-1 RT

These results demonstrate clearly that a 4' substituent is able to edit the interactions of the protein with the sugar-phosphate backbone. Mutations of the protein at these crucial sites should therefore have a significant effect on the ability of the HIV-1 RT to elongate the 4'-acetylated primer. Met184 is located at the tip of the β sheets $\beta 9$ – $\beta 10$ of HIV-1 RT and is in close vicinity to the deoxyribose moiety of the terminal nucleotide of the primer strand (Figure 1) [4,5,7]. It is known that a variation at codon 184 has a significant effect on the efficiency of the DNA synthesis [7]. A suitable mutant is the Met184→Val mutant that has been studied extensively and confers resistance to the nucleoside analogue 3'-thiacytidine (3TC) [15]. The substitution of methionine to the less bulkier valine [7] places the sidechain of the amino acid 184 at a more favorable distance to the deoxyribose moiety of the primer terminus. Indeed, the Met184→Val mutant [16] elongated the 4'-modified primer end with higher efficiency than the wild-type RT (Figures 3b and 4b). Quantification of every single elongation step was investigated as described above and revealed that the addition of the first nucleotide to the modified primer terminus is no longer the rate-limiting step (Table 2).

In comparison with the wild-type HIV-1 RT (Table 1), the Met184→Val mutant elongates the modified primer

Figure 5

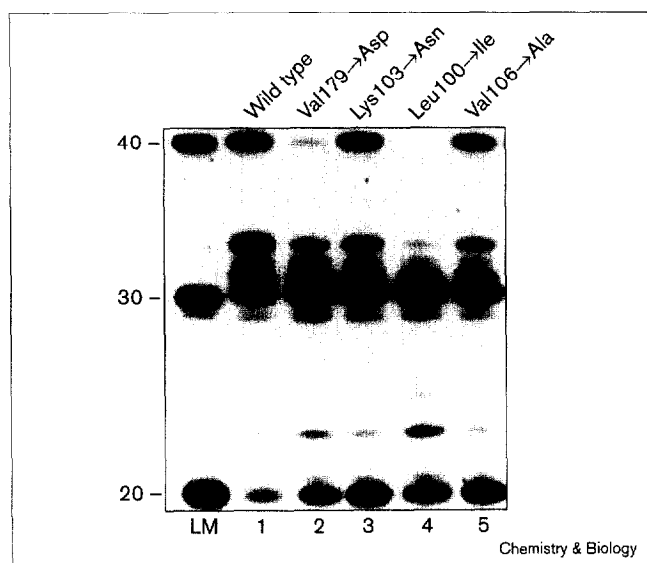
Interactions of the backbone modification with HIV-1 RT. The primer strand is red, the 4'-backbone modified thymidine is gold (the 4'-substituent is illustrated as a ball), and the nearest structural elements of the enzyme are shown as a blue C α trace. The figure

illustrates the translocation of the primer strand and the different protein interactions with the 4' substituent at the 3'-primer end, and at positions 2, 3 and 4, respectively, from the 3'-end (a–d).

Table 2**Efficiency of DNA elongation catalyzed by the HIV-1 RT (Met184→Val) mutant.**

Entry	Elongation event	V_{\max}/K_M
1	30→31	7.9×10^{-1}
2	31→32	3.4×10^{-2}
3	32→33	6.5×10^{-1}
4	33→34	1.1×10^{-2}

strand with a 200-fold higher efficiency (V_{\max}/K_M), whereas the efficiency for natural substrates remains almost the same [15] or is only slightly enhanced [7]. These studies support the assumptions that Met184 makes extensive contacts with the sugar moiety of the nucleotide at the 3' end of the primer and plays a crucial role in the alignment of the primer–template in the catalytic site of the DNA polymerase.

Figure 6

Effect of 4'-modified thymidine triphosphate on DNA strand synthesis catalyzed with mutants of HIV-1 RT. Shown is an autoradiogram of an 11% denaturing PAGE. The numbers on the left side indicate the length of oligonucleotide synthesized in primer extension. LM, line marker. Lane 1, 20-base DNA ^{32}P -5'-end labelled primer (15 nM, 5'-d(GTGGTGCGAATTCTGTGGAT)) and 40-base DNA template (45 nM, 5'-d(TCGGTCGTTTCATCCTTGCTGATCCACAGAAATTCGC-ACCAC)), dATP, dGTP, dCTP (2 μM each), and the modified thymidine triphosphate (100 μM) incubated at 37°C for 150 min with HIV-1 RT (0.2 U/ μl); lane 2, same as in lane 1, but with HIV-1 RT (Val179→Asp); lane 3, same as in lane 1, but with HIV-1 RT (Lys103→Asn); lane 4, same as in lane 1, but with HIV-1 RT (Leu100→Ile); lane 5, same as in lane 1, but with HIV-1 RT (Val106→Ala).

Resistance of HIV to inhibition by non-nucleoside inhibitors of HIV-1 RT arises within a few viral replication cycles upon treatment with a single inhibitor [17,18]. The non-nucleoside-resistance mutations are located around the inhibitor-binding pocket [19]. Two major regions where these mutations occur are the β sheets containing $\beta 9$, $\beta 10$ and $\beta 6$, and the loop between $\beta 5\text{b}$ and $\beta 6$. These regions include mutations Leu100→Ile, Lys103→Asn, Val106→Ala and Val179→Asp. The structural basis of the resistance to non-nucleoside inhibitors remains unclear as no structures of mutant HIV-1 RT bound with an inhibitor and DNA are known [19,20]. To monitor conformational changes of the mutated HIV-1 RT we evaluated their action on the backbone-modified thymidine analog. Incubation of HIV-1 RT with the DNA 5'- ^{32}P -labelled 20-base primer/40-base template complex was performed as described above. The reactions with mutation in the crucial positions of HIV-1 RT [16] resulted in different band patterns to those of the wild-type enzyme (Figure 6). This indicates that the 4'-modified nucleotide recognizes conformational differences within the DNA polymerase cleft and demonstrates that these mutations influence the conformation and orientation of the motifs of the HIV-1 RT that are crucial for alignment of the DNA substrate in the enzyme cleft. These changes might influence the ability of the inhibitor to bind in the binding pocket and confer the apparent resistance.

Significance

Recently, the reverse transcriptase (RT) of the human immunodeficiency virus type 1 (HIV-1) has been studied extensively and crystal structure analyses and studies of mutants have increased our understanding about its structure and function. We have developed a new methodology to monitor the interplay of HIV-1 RT with its DNA substrate. In order to probe the protein interactions with its DNA substrate the sugar backbone of a nucleotide was modified and the efficiency of chain elongation was measured. The backbone substituent acts as an 'antenna' and gives information on the distances between the nucleotides and the amino acids at different positions. This method offers a new and useful tool to derive structural information from kinetic experiments. By applying the technique to other reverse transcriptases or DNA polymerases, structural information about these enzymes in their active form might be deduced. The method is very flexible and the polarity, as well as the position, of the substituent at the sugar can be varied.

Materials and methods

Primer-extension reactions

The 5'-end-labelled 20-base oligonucleotide primer was annealed to its complementary site on a 40-base oligonucleotide by heating the DNA primer to 80°C for 5 min and subsequent cooling to 25°C within 1 h in the reaction buffer (20 mM Tris-HCl (pH 7.5), 6 mM MgCl_2 , 40 mM KCl, 0.5 mM DTT). The reactions were performed as described previously [12]. DNA sequences, nucleotide concentrations and enzyme amounts are given in Figures 3 and 6. The reactions were stopped by addition of formamide and subsequent heating to 90°C and analyzed with an 11%

polyacrylamide denaturing sequencing gel (National Diagnostics). After electrophoresis the gel was transferred to filter paper (Whatmann 3MM) and dried at 80°C. The radioactivity in the DNA bands was quantified using a PhosphorImager (Molecular Dynamics).

Steady-state kinetic assay

The incorporation of the first nucleotide after the incorporated 4'-acetylated nucleotide was measured through incubation of a 5'-³²P-end-labelled 29-base primer (73 fmol, 5'-d(GTGGTGCGAATTCTGTGGATCAGCAAGGA)/40-base DNA template (230 fmol) template complex with HIV-1 RT (0.05 U) under saturating concentrations of 4'-acetyl thymidine triphosphate (200 µM) and various concentrations of dGTP in a final volume of 10 µl. In a typical experiment only up to 20% of the primer was consumed during the reaction (data not shown). The kinetic constants K_M and V_{max} and the substrate efficiency (V_{max}/K_M) were determined for each reaction from quantification of the radioactivity in the bands at the desired nucleotide incorporation sites and the bands one position prior as described previously [13,14]. The kinetic parameters derived from the translocation of the 4'-modification through the enzyme cleft during the DNA polymerization pathway were obtained by standing-start polymerization reactions. The DNA substrates containing the 4'-backbone modifications (T*) at positions 2, 3, and 4, respectively, from the 3'-end of the primer strand were synthesized chemically via the phosphoamidite approach as described recently [11]. DNA sequences of the 5'-³²P-end labelled primers are: 31mer: 5'-d(GTGGTGCGAATTCTGTGGATCAGCAAGGAT*G), 32mer: 5'-d(GTGGTGCGAATTCTGTGGATCAGCAAGGAT*GA), 33mer: 5'-d(GTGGTGCGAATTCTGTGGATCAGCAAGGAT*GAA). The primers were annealed to the appropriate 40-base DNA template and the reactions were performed in the presence of a single deoxynucleotide triphosphate (dNTP). The reactions resulted in the increased accumulation of extended primer as the dNTP concentration was increased. In a typical experiment only up to 20% of the primer was consumed during the reaction (data not shown). The kinetic constants K_M and V_{max} and the substrate efficiency (V_{max}/K_M) were determined as described above.

Enzyme preparations

The expression vectors for the HIV-1 RT p66 mutants were kindly provided by S.H. Hughes (NCI-Frederick Cancer Research and Development Center) and purified as described previously [16]. Enzyme activities were determined as described previously [16].

Acknowledgements

The authors gratefully acknowledge financial support from the Swiss National Science Foundation (NF AIDS program 3139-047297-96, NF 20-9504-96 and NF 31-46768.96) and the Novartis AG. This work was supported by the TMR grant ERBMRXCT 970125 to U.H., by the CNR-target project on Biotechnology and by an ISS-AIDS fellowship to G.M.

References

- Luciw, P. (1996). Human immunodeficiency viruses and their replication. In *Fundamental Virology* (Fields, B.N., Knipe, D.M. & Howley, P.M., eds) pp. 845-916. Lippincott-Raven, New York.
- Hübscher, U. & Spadari, S. (1994). DNA replication and chemotherapy. *Physiol. Rev.* **74**, 259-304.
- Kohlstaedt, L.A., Wang, J., Friedman, J.M., Rice, P.A. & Steitz, T.A. (1992). Crystal structure at 3.5 Å resolution of HIV-1 reverse transcriptase complexed with an inhibitor. *Science* **256**, 1783-1790.
- Jacobo-Molina, A., et al. & Arnold, E. (1993). Crystal structure of human immunodeficiency virus type 1 reverse transcriptase complexed with double-stranded DNA at 3.0 Å resolution shows bent DNA. *Proc. Natl Acad. Sci. USA* **90**, 6320-6324.
- Huang, H., Chopra, R., Verdine, G.L. & Harrison, S.C. (1998). Structure of a covalently trapped catalytic complex of HIV-1 reverse transcriptase: implications for nucleoside analog drug resistance. *Science* **282**, 1669-1675.
- Patel, P.H., et al. & Arnold, E. (1995). Insights into DNA polymerization mechanisms from structure and function analysis of HIV-1 reverse transcriptase. *Biochemistry* **34**, 5351-5363.
- Pandey, V.N., et al. & Modak, M.J. (1996). Role of methionine 184 of human immunodeficiency virus type-1 reverse transcriptase in the polymerase function and fidelity of DNA synthesis. *Biochemistry* **35**, 2168-2179.
- Wilson, J.E., et al. & Furmann, P.A. (1996). Human immunodeficiency virus type-1 reverse transcriptase. Contribution of Met-184 to binding of nucleoside 5'-triphosphate. *J. Biol. Chem.* **271**, 13656-13662.
- Wöhrl, B.M., et al. & Goody, R.S. (1997). Kinetic analysis of four HIV-1 reverse transcriptase enzymes mutated in the primer grip region of p66. Implications for DNA synthesis and dimerization. *J. Biol. Chem.* **272**, 17581-17587.
- Ghosh, M., Williams, J., Powell, M.D., Levin, J.G. & Le Grice, S.F.J. (1997). Mutating a conserved motif of the HIV-1 reverse transcriptase palm subdomain alters primer utilization. *Biochemistry* **36**, 5758-5768.
- Marx, A., et al. & Giese, B. (1996). Synthesis of 4'-C-acylated thymidines. *Helv. Chim. Acta* **79**, 1980-1994.
- Marx, A., MacWilliams, M.P., Bickle, T.A., Schwitter, U. & Giese, B. (1997). 4'-Acylated thymidines: a new class of DNA chain terminators and photocleavable building blocks. *J. Am. Chem. Soc.* **119**, 1131-1132.
- Randall, S.K., Eritja, R., Kaplan, B.E., Petruska, J. & Goodman, M.F. (1987). Nucleotide insertion kinetics opposite abasic lesions in DNA. *J. Biol. Chem.* **262**, 6864-6870.
- Boosalis, M.S., Petruska, J. & Goodman, M.F. (1987). DNA polymerase insertion fidelity: gel assay for site-specific kinetics. *J. Biol. Chem.* **262**, 14689-14696.
- Wainberg, M.A., et al. & Prasad, V.R. (1996). Enhanced fidelity of 3TC-selected mutant HIV-1 reverse transcriptase. *Science* **271**, 1282-1285.
- Maga, G., Amacker, M., Tuel, N., Hübscher, U. & Spadari, S. (1997). Resistance to nevirapine of HIV-1 reverse transcriptase mutants: loss of stabilizing interactions and thermodynamic or steric barriers are induced by different single amino acid substitutions. *J. Mol. Biol.* **274**, 738-747.
- Nunberg, J.H., et al. & Goldman, M.E. (1991). Viral resistance to human immunodeficiency virus type 1-specific pyridone reverse transcriptase inhibitors. *J. Virol.* **65**, 4887-4891.
- Mellors, J.W., et al. & Cheng, Y.C. (1992). In vitro selection and molecular characterization of human immunodeficiency virus-1 resistant to non-nucleoside inhibitors of reverse transcriptase. *Mol. Pharmacol.* **41**, 446-451.
- Tantillo, C., et al. & Arnold, E. (1994). Locations of anti-AIDS drug binding sites and resistance mutations in the three-dimensional structure of HIV-1 reverse transcriptase. Implications for mechanisms of drug inhibition and resistance. *J. Mol. Biol.* **243**, 369-387.
- Das, K., et al. & Arnold, E. (1996). Crystal structure of 8-Cl and 9-Cl TIBO complexed with wild-type HIV-1 RT and 8-Cl TIBO complexed with the Tyr181Cys HIV-1 RT drug resistance mutant. *J. Mol. Biol.* **264**, 1085-1100.
- Gerber, P.R. & Müller, K. (1995). MAB, a generally applicable molecular force field for structure modeling in medicinal chemistry. *J. Comput. Aided Mol. Design* **9**, 251-268.
- Mohamadi, F., et al. & Still, W.C. (1990). MacroModel – an integrated software system for modeling organic and bioorganic molecules using molecular mechanics. *J. Comput. Chem.* **11**, 440-467.
- Weiner, S.J., et al. & Weiner, P.A. (1984). A new force field for molecular mechanical simulations of nucleic acids and proteins. *J. Am. Chem. Soc.* **106**, 765-784.

Because Chemistry & Biology operates a 'Continuous Publication System' for Research Papers, this paper has been published via the internet before being printed. The paper can be accessed from <http://biomednet.com/cbiology/cmb> – for further information, see the explanation on the contents pages.